

Molecular diffusion on a time scale between nano- and milliseconds probed by field-cycling NMR relaxometry of intermolecular dipolar interactions: Application to polymer melts

Markus Kehr

Sektion Kernresonanzspektroskopie, Universität Ulm, 89069 Ulm, Germany

Nail Fatkullin

Department of Physics, Kazan State University, Kazan 420008, Tatarstan, Russia

Rainer Kimmich

Sektion Kernresonanzspektroskopie, Universität Ulm, 89069 Ulm, Germany

(Received 25 September 2006; accepted 29 December 2006; published online 2 March 2007)

A formalism is presented permitting the evaluation of the relative mean-squared displacement of molecules from the intermolecular contribution to spin-lattice relaxation dispersion of dipolar coupled spins. The only condition for the applicability is the subdiffusive power law character of the time dependence of the mean-squared displacement as it is typical for the chain mode regime in polymer liquids. Using field-cycling NMR relaxometry, an effective diffusion time range from nano- to almost milliseconds can be probed. The intermolecular spin-lattice relaxation contribution can be determined with the aid of isotopic dilution, that is, mixtures of undeuterated and deuterated molecules. Experiments have been performed with melts of polyethyleneoxide and polybutadiene. The mean-squared segment displacements have been evaluated as a function of time over five decades. The data can be described by a power law. The extrapolation to the much longer time scale of ordinary field-gradient NMR diffusometry gives good coincidence with literature data. The total time range thus covers nine decades. © 2007 American Institute of Physics.

[DOI: 10.1063/1.2435357]

I. INTRODUCTION

Polymer chain dynamics may be subdivided into three time regimes: local motions, chain modes, and global motions.¹ Local motions are characterized by the segment fluctuation time τ_s . On the other hand, the so-called terminal chain relaxation time τ_t indicates the onset of the dominance of global center-of-mass motions. For the chain mode regime in between, $\tau_s \ll t \ll \tau_t$, model theories predict anomalous power laws for the time dependence of the mean-squared segment displacement which are often taken to be indicative for the model assumptions.¹⁻⁴ It is therefore of interest to probe the mean-squared segment displacement in a time range as wide as possible.

NMR techniques based on gradients of the main field or of the radio frequency field permit diffusivity measurements over four orders of magnitude, that is, for low-molecular liquids typically from 100 μ s to 1 s, as recently demonstrated in Ref. 5. In the following, we anticipate subdiffusive power laws⁶ for the time dependence of the mean-squared displacement

$$\langle \tilde{r}^2 \rangle = \tilde{b}^2 \left(\frac{t}{\tau_s} \right)^\alpha \quad (0 < \alpha < 1), \quad (1)$$

where \tilde{b} is a characteristic length, which in low-molecular liquids is of the order of the molecular size, and in the case of polymer liquids is of the order of the Kuhn segment length. τ_s is a molecular fluctuation time. This sort of mean-

squared displacement law typically occurs in polymer liquids on a time scale shorter than the terminal relaxation time.^{1,2}

On the basis of this crucial power law assumption, we now report a NMR measuring protocol supplementary to ordinary field-gradient NMR diffusometry. It permits the access to five more decades at shorter times, i.e., from nanoseconds to hundreds of microseconds. This time scale is conjugated to the frequency range probed with field-cycling NMR relaxometry,⁷ which ranges from kilohertz up to several hundreds of megahertz of conventional NMR spectrometers.

Intermolecular dipolar interaction is modulated primarily by translational displacements of molecules *relative* to each other. With respect to entangled polymers, this gives rise to another motivation for doing this sort of experiments: An essential question for our understanding of polymer chain dynamics is whether and to what degree neighboring chains move independently of each other. Any correlations are expected to affect the time dependence of the relative mean-squared segment displacement.

The principle of the technique to be outlined in the following is to evaluate the mean-squared displacement from the spin-lattice relaxation rate caused by intermolecular dipolar interactions. The intermolecular spin-lattice relaxation rate can be determined with the aid of a series of isotopic dilution experiments, where one anticipates that there is no other isotopic effect than the modification of dipolar cou-

plings among spins.^{8,9} With proton resonance, this refers to undeuterated molecules dispersed in a matrix of deuterated molecules of the same chemical species.

The spin-lattice relaxation rate of protons in diamagnetic liquids is usually governed by fluctuating dipole-dipole interactions. It is consequently composed of inter- and intramolecular contributions (see Refs. 1, 8, and 10, for example). The Hamiltonian of dipolar interaction between protons (“H”) and deuterons (“D”) is lowered by the quotient of the gyromagnetic ratios, $\gamma_D/\gamma_H \approx 0.15$, relative to proton-proton couplings. The intermolecular dipolar spin-lattice relaxation rate of proton-deuteron pairs is diminished by the square of this factor, i.e., by a factor of about 0.023. Although the influence of proton-deuteron dipolar interaction is relatively weak, we will consider it explicitly (see Appendix) and take it into account for the sake of rigor.

It will be shown that the relative mean-squared displacement can be evaluated from intermolecular spin-lattice relaxation rates provided that it obeys a subdiffusive time dependence [see Eq. (1)] with $\alpha < 2/3$. Apart from this, there is no restriction with respect to the type or size of the molecules under consideration. The detailed treatment of this idea and its experimental demonstration is the main objective of this paper.

II. EXPERIMENT

Poly(ethylene oxide) (PEO) and polybutadiene (PB) were purchased from PSS (Polymer Standard Service, Mainz, Germany). The degree of deuteration of the perdeuterated polymers was specified as 98%. The weight average molecular weight of undeuterated and deuterated PEOs were $M_w = 178\,000$ and $132\,000$, respectively. The polydispersities were 1.09 and 1.07, respectively. The polydispersities of PB were 1.02 ($M_w = 196\,000$, undeuterated) and 1.03 ($M_w = 191\,000$, perdeuterated). No molecular weight dependence was found with both the field-cycling relaxometry and field-gradient diffusometry experiments.

A series of mixtures of undeuterated and deuterated polymers in different concentrations was prepared. The objective was to permit the extrapolation of the proton spin-lattice relaxation rate to concentration zero of the undeuterated polymers. In this way, the true intramolecular spin-lattice relaxation rate can be determined. Note that this sort of evaluation eliminates not only residual intermolecular contribution but also effects of imperfections in the molecular mixing and isotopic dilution.

Undeuterated and deuterated polymers were mixed by first dissolving them in chloroform (CHCl_3) and mixing the solutions by shaking or stirring for about 3 days. The solvent was then evaporated at 70°C with the aid of a rotary evaporator.

The proton spin-lattice relaxation dispersion was studied with the aid of the field-cycling NMR relaxometry technique.⁷ A field cycle consists of relaxation, detection, and polarization (equal to recycle delay) intervals. In the fixed polarization interval, the magnetic field is as high as permitted by the duty cycle of the magnet. After the Curie magnetization of the nuclear dipoles is reached, the field is

switched to a variable relaxation field where the magnetization relaxes towards the new equilibrium value. The relaxation curve is recorded point by point by switching to the fixed detection field after a variable relaxation delay and “reading” the magnetization at the end of the relaxation interval with the aid of a 90° radio frequency pulse. In this way, the spin-lattice relaxation time can be measured over several decades of the magnetic flux density (or frequency).

A Stellar relaxometer covering frequencies in the range of 1 kHz–30 MHz was employed. The frequency range was supplemented by two conventional NMR spectrometers operating at 4.7 and 9.4 T, respectively. The field-cycling relaxometer is equipped with homemade auxiliary coils for the compensation of the earth field and stray fields from other magnets in the laboratory. The precision of the field cycles was checked with the aid of a fast Hall teslameter (Projekt Elektronik FM 210) probing the flux density at the sample position during test field cycles. The measuring bandwidth of the teslameter is 35 kHz, and the resolution is 0.01 mT. Within the experimental error, all relaxation curves could be described by monoexponential functions over about one decade of the signal amplitude. In each experiment, all data have been measured twice by varying the frequency from high to low values and the other way round. The same values were found. Typical experimental errors were a few percent, and did not exceed 3% under the most unfavorable conditions.

The intermolecular spin-lattice relaxation rate was evaluated from isotopically diluted systems, i.e., undeuterated molecules dispersed in a matrix of deuterated molecules of the same species based on the formalism described below. The concentration of undeuterated molecules was varied, and the measured spin-lattice relaxation rates were extrapolated to concentration zero. In this way, intra- and intermolecular rate contributions can be identified and evaluated.

III. EVALUATION THEORY

Mixtures of undeuterated and deuterated molecules of any concentration ratio are considered. Let φ_H be the fraction of undeuterated hydrogen atoms so that $\varphi_D = 1 - \varphi_H$ is the fraction of the deuterated counterparts. In a system consisting of a single diamagnetic phase, proton relaxation curves can be described by a monoexponential function, and spin-lattice relaxation is usually dominated by dipolar coupling. Under such conditions the spin-lattice relaxation rate can be split into two terms as follows:

$$\frac{1}{T_1^{\text{tot}}(\omega_H, \varphi_H)} = \frac{1}{T_1^{\text{intra}}(\omega_H, \varphi_H)} + \frac{1}{T_1^{\text{inter}}(\omega_H, \varphi_H)}, \quad (2)$$

where ω_H is the proton resonance angular frequency and $1/T_1^{\text{intra}}(\omega_H, \varphi_H)$ and $1/T_1^{\text{inter}}(\omega_H, \varphi_H)$ are the spin-lattice relaxation rates caused by intra- and intermolecular dipolar interactions, respectively (see Fig. 1). Since isotopic dilution is expected to have no perceptible effect on molecular dynamics and hence on the intramolecular proton relaxation rate,

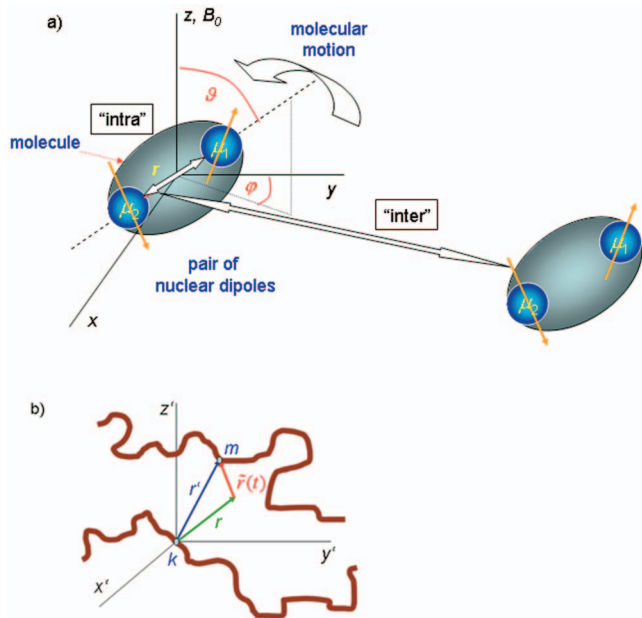


FIG. 1. (Color) Schematic representations of intra- and intermolecular dipolar couplings of spin pairs. (a) Intramolecular interactions are modulated by rotational diffusion described by polar coordinates φ , ϑ , and r of the internuclear vector \mathbf{r} . Intermolecular couplings fluctuate due to translational displacements of molecules relative to each other. (b) In polymer liquids, intermolecular interactions refer to segments on different macromolecules.

$$\frac{1}{T_1^{\text{intra}}(\omega_H)} = \frac{1}{T_1^{\text{intra}}(\omega_H, \varphi_H)}, \quad (3)$$

independent of the value of φ_H .

The intermolecular proton spin-lattice relaxation rate is composed of contributions from proton-proton (HH) and proton-deuteron (HD) dipolar couplings. The latter is much weaker but anyway finite. The intermolecular contribution is then

$$\frac{1}{T_1^{\text{inter}}(\omega_H; \varphi_H)} = \frac{1}{T_1^{\text{inter}}(\omega_H; \varphi_H)} + \frac{1}{T_1^{\text{inter}}(\omega_H; \varphi_H)}, \quad (4)$$

where $1/T_1^{\text{inter}}(\omega_H; \varphi_H=1)=0$ and $1/T_1^{\text{inter}}(\omega_H; \varphi_H \rightarrow 0) \rightarrow 0$.

Inserting Eqs. (3) and (4) in Eq. (2) gives

$$\frac{1}{T_1^{\text{tot}}(\omega_H, \varphi_H)} = \frac{1}{T_1^{\text{intra}}(\omega_H)} + \frac{1}{T_1^{\text{inter}}(\omega_H; \varphi_H)} + \frac{1}{T_1^{\text{inter}}(\omega_H; \varphi_H)}. \quad (5)$$

The total relaxation rate for $\varphi_H=1$ (undeuterated system) minus the total relaxation rate for $\varphi_H \ll 1$ (optimally diluted system) is

$$\begin{aligned} & \frac{1}{T_1^{\text{tot}}(\omega_H, \varphi_H=1)} - \frac{1}{T_1^{\text{tot}}(\omega_H; \varphi_H \ll 1)} \\ &= \frac{1}{T_1^{\text{inter}}(\omega_H, \varphi_H=1)} - \frac{1}{T_1^{\text{inter}}(\omega_H; \varphi_H \ll 1)} \\ &= \frac{1}{T_1^{\text{inter}}(\omega_H; \varphi_H \ll 1)}. \end{aligned} \quad (6)$$

That is, the intramolecular contribution has been eliminated,

and the right-hand side of Eq. (6) is merely composed of intermolecular relaxation rates. The derivation of the corresponding expressions requires somewhat lengthy calculations which are described in the Appendix [see Eqs. (A23)–(A26)].

For power laws as given in Eq. (1) for $\alpha < 2/3$, the result for undeuterated systems becomes [Eq. (A23)]

$$\frac{1}{T_1^{\text{inter}}(\omega_H, \varphi_H=1)} = \left(\frac{\mu_0}{4\pi} \right)^2 \frac{16\sqrt{\pi}}{5\sqrt{6}} f_1(\alpha) \frac{\gamma_H^4 \hbar^2 I(I+1) \rho_s}{\omega_H \langle \tilde{r}^2(1/\omega_H) \rangle^{3/2}}, \quad (7)$$

where

$$f_1(\alpha) = \frac{\pi(1 + 2 \times 2^{3\alpha/2})}{2 \cos(3\pi\alpha/4) \Gamma(3\alpha/2)}. \quad (8)$$

$\Gamma(x)$ is the gamma function, $I=1/2$ is the proton spin quantum number, and α is the subdiffusive exponent of the mean-squared displacement law given in Eq. (1). The first term, 1, in the parentheses of the numerator of $f_1(\alpha)$ is related to single quantum transitions of proton spins induced by dipole-dipole interactions, and the second term, $2 \times 2^{3\alpha/2}$, reflects the contribution of double quantum transitions. $\langle \tilde{r}^2(1/\omega_H) \rangle$ is the mean-squared displacement of molecules relative to each other in a time interval $t=1/\omega_H$ determined by the angular frequency of proton resonance. Note that qualitatively the same relationship as Eq. (7) can be derived on the basis of simple scaling arguments. This will be demonstrated in Sec. V.

In isotopically diluted systems, $\varphi_H \ll 1$, the contribution by proton-proton interactions differs from the expression in Eq. (7) only by a factor φ_H : [Eq. (A23)]

$$\begin{aligned} & \frac{1}{T_{1\text{HH}}^{\text{inter}}(\omega_H; \varphi_H \ll 1)} \\ &= \left(\frac{\mu_0}{4\pi} \right)^2 \frac{16\sqrt{\pi}}{5\sqrt{6}} f_1(\alpha) \frac{\gamma_H^4 \hbar^2 I(I+1) \rho_s}{\omega_H \langle \tilde{r}^2(1/\omega_H) \rangle^{3/2}} \varphi_H. \end{aligned} \quad (9)$$

Analogously, for the contribution by deuteron-proton dipolar interactions, we find [Eq. (A25)]

$$\begin{aligned} & \frac{1}{T_{1\text{HD}}^{\text{inter}}(\omega_H; \varphi_H \ll 1)} \\ &= (1 - \varphi_H) \left(\frac{\gamma_D}{\gamma_H} \right)^2 \frac{S(S+1)}{I(I+1)} f_2(\alpha) \frac{1}{T_1^{\text{inter}}(\omega_H, \varphi_H=1)}, \end{aligned} \quad (10)$$

where

$$f_2(\alpha) = \frac{1 + 2(1 + \gamma_D/\gamma_H)^{(3\alpha-2)/2} + (1 - \gamma_D/\gamma_H)^{(3\alpha-2)/2}}{1 + 2 \times 2^{3\alpha/2}}. \quad (11)$$

$S=1$ is the deuteron spin quantum number. The factor $1 - \varphi_H = \varphi_D$ corresponds to the factor φ_H in Eq. (9). The ratio γ_D/γ_H reflects the reduced dipolar magnetic field of deuterons relative to protons. The first term, 1, in the numerator of Eq. (11) reflects single quantum transitions of proton spins

induced by magnetic dipole-dipole interactions with deuteron spins. The second term, $2(1 + \gamma_D/\gamma_H)^{(3\alpha-2)/2}$, is connected to the double quantum transitions of proton and deuteron spins induced by their dipolar interactions. The last term, $(1 - \gamma_D/\gamma_H)^{(3\alpha-2)/2}/3$, is the contribution of flip-flop (or zero-quantum) transitions between proton and deuteron spins.

Using Eqs. (7), (9), and (10), relation (6) can be rewritten as

$$\begin{aligned} \frac{1}{T_1^{\text{tot}}(\omega_H, \varphi_H = 1)} - \frac{1}{T_1^{\text{tot}}(\omega_H; \varphi_H \ll 1)} \\ = \frac{1}{T_1^{\text{inter}}(\omega_H, \varphi_H = 1)} (1 - \varphi_H) \\ \times \left\{ 1 - \left(\frac{\gamma_D}{\gamma_H} \right)^2 \frac{S(S+1)}{I(I+1)} f_2(\alpha) \right\}. \end{aligned} \quad (12)$$

Rearranging Eq. (12) leads to the following final expression of the intermolecular spin-lattice relaxation rate of an undeuterated system:

$$\begin{aligned} \frac{1}{T_1^{\text{inter}}(\omega_H, \varphi_H = 1)} \\ = \frac{1/T_1^{\text{tot}}(\omega_H, \varphi_H = 1) - 1/T_1^{\text{tot}}(\omega_H, \varphi_H \ll 1)}{(1 - \varphi_H) \{ 1 - (\gamma_D/\gamma_H)^2 [S(S+1)/I(I+1)] f_2(\alpha) \}}. \end{aligned} \quad (13)$$

The only parameter in Eq. (13) that is not directly determined by experimental data is the exponent α in the anticipated range [recall Eq. (1)].

Determining $1/T_1^{\text{inter}}(\omega_H, \varphi_H = 1)$ from experimental data according to Eq. (13) permits one to evaluate the mean-squared displacement of molecules relative to each other in a time interval $t = 1/\omega_H$ from Eq. (7) as

$$\begin{aligned} \langle \bar{r}^2(t = 1/\omega_H) \rangle \\ = \left(\left(\frac{\mu_0}{4\pi} \right)^2 \frac{16\sqrt{\pi}}{5\sqrt{6}} f_1(\alpha) \frac{\gamma_H^4 \hbar^2 I(I+1) \rho_s}{\omega_H} \right. \\ \left. \times T_1^{\text{inter}}(\omega_H, \varphi_H = 1) \right)^{2/3}. \end{aligned} \quad (14)$$

If molecules move independently of each other, the mean-squared displacement relative to the laboratory frame is just half the relative mean-squared displacement,

$$\langle R^2(t) \rangle = \frac{1}{2} \langle \bar{r}^2(t) \rangle. \quad (15)$$

Note that the only condition which Eq. (14) anticipates is a subdiffusive mean-squared displacement law according to Eq. (1) with $\alpha < 2/3$. This can be relevant for very different but usually relatively complex systems.^{6,11} Typical examples where subdiffusive mean-squared displacement laws apply are polymer liquids. In the following, we will focus on melts of so-called entangled polymers.

For the evaluation of Eq. (14) one must know the numerical value of the exponent α for the calculation of $f_1(\alpha)$ given in Eq. (8). The typical range predicted by polymer dynamics theories¹⁻³ is $1/4 \leq \alpha \leq 1/2$. This relatively narrow

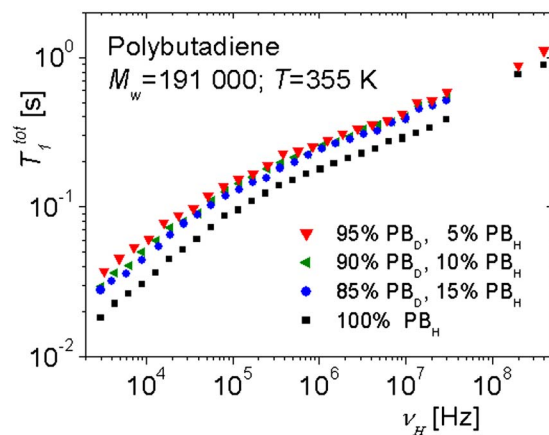


FIG. 2. Primary proton spin-lattice relaxation data vs the frequency $\nu_H = \omega_H/2\pi$ in PB melts with different fractions φ_H of undeuterated chains.

variation width and the low value of $2/3 < 1$ of the power exponent on the right-hand side of Eq. (14) suggest that the precise value of α is not very important. For analytical convenience it may be reasonable to set $\alpha = 1/3$, because we can then use an exact value for the gamma function in Eq. (8), $\Gamma(3\alpha/2) = \Gamma(1/2) = \sqrt{\pi}$. Interestingly $\alpha = 1/3$ is very close to the findings in computer simulations.¹²⁻¹⁴

IV. RESULTS

Figure 2 shows a data set of the proton spin-lattice relaxation times T_1^{tot} in PB melts at various mixture ratios φ_H with the perdeuterated species. Extrapolating data point by point to “infinite” dilution, i.e., $\varphi_H \rightarrow 0$, provides the proton spin-lattice relaxation time $T_1^{\text{tot}}(\omega_H; \varphi_H \rightarrow 0)$ for intramolecular dipolar proton-proton interactions plus intermolecular proton-deuteron dipolar interactions. Note that this extrapolation is not really necessary but is recommendable if appropriate samples are available, since it ensures that any imperfections by incomplete molecular mixing are eliminated. The values for undiluted melts, $T_1^{\text{tot}}(\omega_H; \varphi_H = 1)$, are also given. From these data one can determine the pure intermolecular contribution represented by the spin-lattice relaxation time $T_1^{\text{inter}}(\omega_H, \varphi_H = 1)$ according to Eq. (13) (see Fig. 3), and from this the relative mean-squared segment displacement, as defined by Eq. (14). Figure 4 shows a corresponding plot.

Analogous experiments have been carried out with PEO melts. The mean-squared segment displacement versus time is shown in Fig. 5 in comparison to the data measured with fringe field-gradient NMR diffusometry.¹⁵ The range of the root-mean-squared displacements probed by the technique is roughly 0.5–50 nm, i.e., two orders of magnitude.

V. DISCUSSION AND CONCLUSIONS

The contribution of intermolecular dipolar interaction to spin-lattice relaxation depends on fluctuations due to mutual translational diffusion.^{8,10} Information on molecular diffusion can therefore be derived from isotopic dilution experiments specifically acquiring the intermolecular contribution to spin-lattice relaxation. We have shown that the mean-squared displacement can directly be determined on this ba-

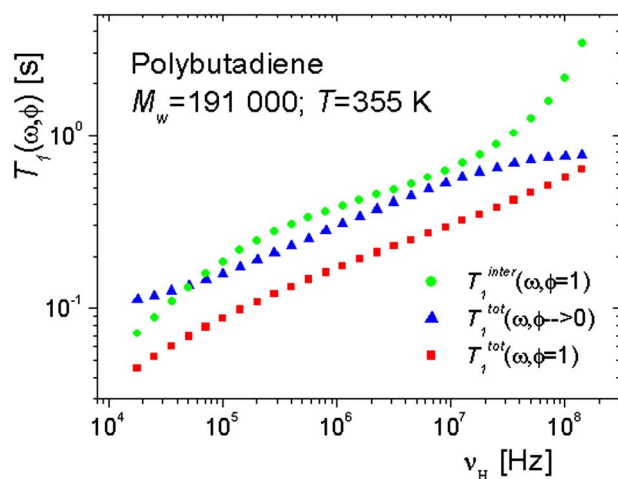


FIG. 3. Frequency dependence ($\nu_H = \omega_H/2\pi$) of the proton spin-lattice relaxation times T_1^{tot} in PB melts after extrapolating the fraction of undeuterated chains to zero, $\varphi_H \rightarrow 0$, and for undiluted melts, $\varphi_H = 1$. From these data, the intermolecular contribution characterized by $T_1^{\text{inter}}(\omega_H, \varphi_H = 1)$ has been evaluated according to Eq. (13) ($\varphi \equiv \varphi_H$).

sis provided that a subdiffusive power law [see Eq. (1)] is valid. In combination with field-cycling NMR relaxometry,⁷ the time dependence of the mean-squared displacement can thus be obtained over many orders of magnitude of time, that is, nano- to almost milliseconds. This time scale is not accessible with other techniques such as field-gradient NMR diffusometry.^{5,16–18} The method presented here can therefore be considered to be supplementary to conventional techniques.

The test experiments were performed with polymer melts, although the method may be suitable for any other system with subdiffusive mean-squared displacement laws. Polymer liquids are particularly suited for this sort of investigation since there is a strong tendency for anomalous segment diffusion properties on a time scale where center-of-mass diffusion does not yet dominate. Under such

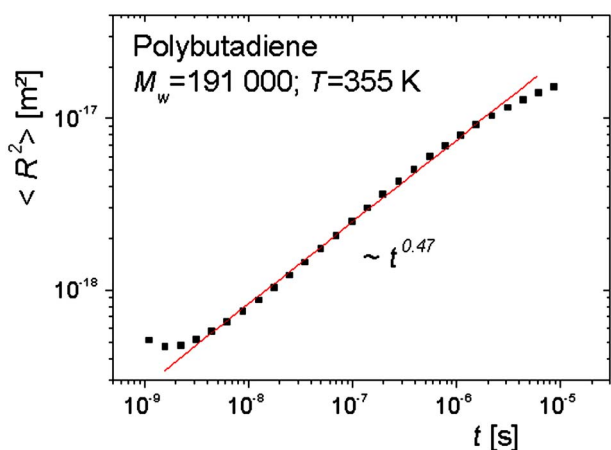


FIG. 4. Mean-squared segment displacement vs diffusion time $t = 1/\omega_H$ in PB melts evaluated from the data in Fig. 3 according to Eqs. (13)–(15). The crossover to a plateau at short times indicates the measuring limit of the technique. The power law given in the plot represents the dispersion in the middle of the experimental time range corresponding to the straight line. A flatter slope appears at times $t > 1 \mu\text{s}$.

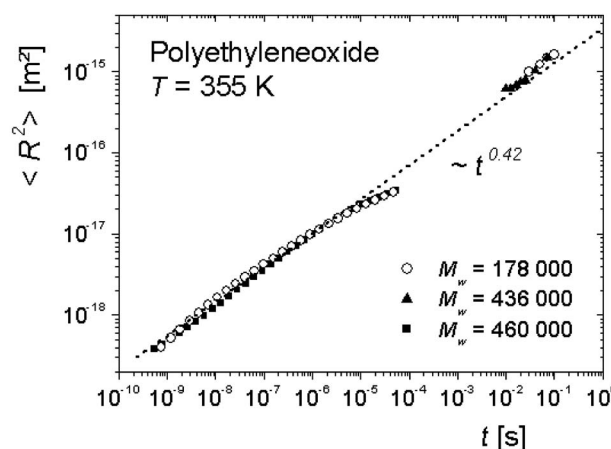


FIG. 5. Mean-squared segment displacement vs diffusion time in PEO melts. The short-time data refer to the relaxometry technique, while those for $t > 10$ ms have been measured with fringe field-gradient NMR diffusometry (Ref. 15). The molecular weights of the undeuterated polymers were $M_w = 178\,000$, $436\,000$, and $460\,000$. The data for the latter are taken from Ref. 15. The relaxation-based data for $M_w = 178\,000$ correspond to the extrapolation $\varphi_H \rightarrow 0$ mentioned above, while those for $M_w = 460\,000$ were directly evaluated from data sets for $\varphi_H = 1$ and $\varphi_H = 0.05$ according to Eqs. (13)–(15). In the frame of these samples, no molecular weight dependence was detected on the whole time scale. The data in the nanosecond range and below indicate the increasing influence of local segment fluctuations which are not affected by intermolecular interactions. The dotted line and its slope tentatively anticipate the validity of a power law in the total range. Note, however, that at about $10 \mu\text{s}$ and above, a crossover to a flatter slope appears, which is not described by the power law shown in the plot.

conditions, a theory has been developed directly providing the mean-squared segment displacement as a function of time [Eq. (14)].

Qualitatively, this relation can also be obtained on the basis of scaling arguments. In our previous work,¹⁹ it was shown that the autocorrelation function for intermolecular dipolar interaction in an undeuterated system varies as

$$G(t) \propto \frac{\rho}{\langle \tilde{r}^2(t) \rangle^{3/2}}, \quad (16)$$

where ρ is the number density of hydrogen atoms. We now assume the subdiffusive mean-squared displacement law given in Eq. (1) in the time range $\tau_s < t < \tau_l$ relevant for segment diffusion in polymer liquids, where τ_s and τ_l are the shortest and longest chain mode relaxation times, respectively.^{1–3} The frequency dependence of the intermolecular contribution to the proton spin-lattice relaxation rate scales according to the Fourier transform of Eq. (16), i.e.,

$$\begin{aligned} \frac{1}{T_1^{\text{inter}}(\omega_H, \varphi_H = 1)} &\propto \int_0^\infty \frac{\rho}{\langle \tilde{r}^2(t) \rangle^{3/2}} \cos(\omega_H t) dt \\ &\propto \frac{\rho}{\omega \langle \tilde{r}^2(1/\omega_H) \rangle^{3/2}}, \end{aligned} \quad (17)$$

where we have anticipated $\alpha < 2/3$. The diffusion time can be set as $t = 1/\omega_H$ since at angular frequencies $\omega_H \gg 1/\tau_l$, the main contribution to the right-hand side of Eq. (17) comes from times of the order $t \approx 1/\omega_H$. The simple scaling relation given in Eq. (17) thus permits one to extract the time dependence of the relative mean-squared segment displacement from the frequency dependence of the intermolecular contri-

bution to spin-lattice relaxation rate according to

$$\langle \tilde{r}^2(t = 1/\omega_H) \rangle \propto \left(\frac{\rho T_1^{\text{inter}}(\omega_H, \varphi_H = 1)}{\omega_H} \right)^{2/3}, \quad (18)$$

in accordance with Eq. (14). The intermolecular relaxation rate can be determined by isotopic dilution, as described above and in the Appendix.

In principle, the time limits of the isotopic dilution experiments evaluated here are determined by the field-cycling NMR relaxometry technique. The low-frequency limit, that is, the extent of the application range at long times, is determined either by local fields⁷ or by the spin-lattice relaxation dispersion cutoff at $\omega_H \approx 1/\tau_i$, as mentioned before. For polymers with large enough molecular weights, as it is the case in the present study, this limitation can be ruled out. We therefore conclude that the low-field limitation is given by local fields starting to dominate the external magnetic field. This is a system dependent effect that may be influenced by the choice of the sample material. With polymer melts, the limit $\omega_H \gg 1/\tau_i$ on the one hand, and the empirical inequality¹ $M_w > 60\,000$ on the other will provide the best compromise in the sense of the application range at long times. A time range up to milliseconds thus becomes realistic.

The short-time limit is again determined by two factors. The highest switchable magnetic field achievable with field-cycling magnet coils restricts the technique to about $\nu_H \leq 4 \times 10^7$ Hz. The experimental accuracy becomes worse when approaching this limit, while conventional NMR spectrometers are often only available for much higher frequencies. Then another condition may be violated, namely, the limit $\omega_H \leq 1/\tau_s$. That is, local motions start to dominate spin-lattice relaxation, and intermolecular interactions become irrelevant. In the case of the polymer species considered in the present study, a short-time limit of nanoseconds appears to be typical. In this time range, the evaluated time dependence of the mean-squared displacement consequently disappears (see Fig. 4) as a manifestation of the experimental measuring limit.

APPENDIX: INTERMOLECULAR SPIN-LATTICE RELAXATION RATES IN BLENDS OF UNDEUTERATED AND DEUTERATED MOLECULES

Let us first consider the intermolecular contribution to the spin-lattice relaxation rate by homonuclear dipolar interaction of protons in a system with a proton fraction φ_H . Based on the general Bloembergen-Purcell-Pound theory,^{8,10} we have

$$\frac{1}{T_{1\text{HH}}^{\text{inter}}(\omega_H, \varphi_H)} = \left(\frac{\mu_0}{4\pi} \right)^2 \frac{\gamma_H^4 \hbar^2 I(I+1)}{2} [j^{(1)}(\omega_H) + j^{(2)}(2\omega_H)]. \quad (A1)$$

The spectral densities $j^p(\omega)$ are defined by the following series of relations:

$$j^{(p)}(\omega) = 2 \operatorname{Re} \int_0^\infty G^{(p)}(t) \exp\{-i\omega t\} dt, \quad (A2)$$

$$G^{(p)}(t) = \sum_m^{\text{inter}} \langle F_{km}^{(p)}(t) F_{km}^{(p)*}(0) \rangle, \quad (A3)$$

$$F_{km}^{(p)}(t) = d_p Y_{2p}(\mathbf{e}_{km}(t)) / r_{km}^3(t), \quad (A4)$$

$$d_0^2 = \frac{16\pi}{5}, \quad d_1^2 = \frac{8\pi}{15}, \quad d_2^2 = \frac{32\pi}{15}, \quad (A5)$$

$$\mathbf{e}_{km}(t) = \mathbf{r}_{km}(t) / r_{km}(t). \quad (A6)$$

The brackets in expression (A3) denote an ensemble average over all pairs of proton dipoles k and m on different molecules. $\mathbf{r}_{km}(t)$ is the time dependent internuclear vector [see Fig. 1(b)] connecting the k th and the m th proton, and Y_{lp} is the p th component of spherical harmonics of rank l normalized to unity.

Stripped of all constant coefficients, the autocorrelation functions can be expressed as

$$A_p(t) = \sum_m^{\text{inter}} \left\langle \frac{Y_{2p}(\mathbf{e}_{km}(t))}{r_{km}^3(t)} \frac{Y_{2p}^*(\mathbf{e}_{km}(0))}{r_{km}^3(0)} \right\rangle. \quad (A7)$$

The initial and final internuclear distance vectors of an intermolecular proton spin pair will now be called \mathbf{r} and \mathbf{r}' , respectively [see Fig. 1(b)]. The propagator of relative motions of the two protons is by definition the conditional distance probability density $\tilde{W}(\mathbf{r}, \mathbf{r}'; t)$. That is, $\tilde{W}(\mathbf{r}, \mathbf{r}'; t) d^3 r'$ is the conditional probability that the final internuclear distance vector \mathbf{r}' points in the volume element $d^3 r'$ if the initial distance vector was \mathbf{r} . Furthermore let $p(r)$ be the *a priori* probability density for the initial internuclear distance vector \mathbf{r} . The *a priori* probability that \mathbf{r} points in the volume element $d^3 r$ is then given by $p(r) d^3 r = n g(r) d^3 r$, where n^{-1} is the mean volume per proton spin and $g(r)$ is the intermolecular radial distribution function taking into account the average excluded volume. In the case of macromolecules, $g(r)$ is considered as the average over all segments of a chain. The expression $p(r) \tilde{W}(\mathbf{r}, \mathbf{r}'; t) d^3 r d^3 r' = n g(r) \tilde{W}(\mathbf{r}, \mathbf{r}'; t) d^3 r d^3 r'$ is then the probability that the initial internuclear distance vector points in the volume element $d^3 r$ and the final internuclear distance vector in $d^3 r'$.

On this basis, the time dependent correlation function $A_p(t)$ can be expressed as

$$A_p(t) = n \int \int \frac{d^3 r}{r^3} \frac{d^3 r'}{r'^3} g(r) Y_{2p}(\mathbf{e}) Y_{2p}^*(\mathbf{e}') \tilde{W}(\mathbf{r}, \mathbf{r}'; t). \quad (A8)$$

For isotropic and spatially homogeneous liquids, the conditional probability density will depend merely on the relative displacement $\mathbf{r}' - \mathbf{r}$ in the interval t . Together with the radial distribution function, this stipulates

$$\tilde{W}(\mathbf{r}, \mathbf{r}'; t) = \tilde{W}(\mathbf{r}' - \mathbf{r}; t)g(r'). \quad (\text{A9})$$

For convenience, the conditional probability density can be represented in Fourier representation as follows:

$$\tilde{W}(\mathbf{r}' - \mathbf{r}; t) = \int \frac{d\mathbf{k}}{(2\pi)^3} \tilde{A}(k^2; t) \exp\{i\mathbf{k} \cdot (\mathbf{r} - \mathbf{r}')\}, \quad (\text{A10})$$

where $\tilde{A}(k^2; t)$ is the spatial Fourier transform of $\tilde{W}(\mathbf{r}' - \mathbf{r}; t)$ and \mathbf{k} is the wave vector, that is, the variable conjugate to $\mathbf{r}' - \mathbf{r}$. Due to the isotropy of the system, the time dependent function $\tilde{A}(k^2; t)$ depends only on the magnitude of the wave vector \mathbf{k} . Note that $\tilde{A}(k^2; t)$ can also be designated as the intermolecular incoherent dynamical structure factor in the reference frame moving with the considered molecule (or a segment of the so-called tagged polymer chain) in analogy to the usual van Hove incoherent dynamical structure factor defined in the laboratory frame.

The exponential function in Eq. (A10) can be expanded in terms of Bessel functions $J_{l+1/2}(x)$ and spherical harmonics $Y_{lp}(x)$ according to

$$\exp\{i\mathbf{k} \cdot \mathbf{r}\} = 4\pi \sqrt{\frac{\pi}{2kr}} \sum_{l,p} i^l J_{l+1/2}(kr) Y_{lp}^*(\mathbf{k}/k) Y_{lp}(\mathbf{r}/r). \quad (\text{A11})$$

Inserting Eqs. (A9)–(A11) in Eq. (A8) and integrating the right-hand side lead to

$$A_p(t) = n \int_0^\infty \tilde{A}(k^2; t) k dk \left[\int_0^\infty g(r) \frac{J_{5/2}(kr)}{r^{3/2}} dr \right]^2, \quad (\text{A12})$$

where we have exploited the orthonormal properties of spherical harmonics.

For our purposes, the radial distribution function can be approximated by

$$g(r) = \begin{cases} 1 & \text{for } r > \sigma \\ 0 & \text{for } r \leq \sigma, \end{cases} \quad (\text{A13})$$

where σ is the radius of the first coordination shell of the molecule under consideration. The justification for this crude approximation is that only relatively low frequencies, i.e., long times, are of interest. In the case of polymers, the time scale of interest is $t \gg \tau_s$, where τ_s is the segment fluctuation time. The wave numbers probed by translational diffusion on these time scales are then low enough to satisfy $k\sigma \ll 1$. That is, microstructural details on the length scale of σ are taken to be unimportant.

On this basis, the integral in Eq. (A12) can exactly be evaluated as

$$\int_0^\infty \frac{J_{5/2}(kr)}{r^{3/2}} dr = \frac{\sqrt{k}}{(k\sigma)^{3/2}} J_{3/2}(k\sigma). \quad (\text{A14})$$

The Bessel function can be approximated by $J_{3/2}(x) \equiv \sqrt{2/9\pi} x^{3/2}$ in the limit $x \ll 1$. That is, the expression becomes independent of σ in the relevant low wave number limit. Equation (A12) thus becomes

$$A_p(t) = \frac{2}{9\pi} n \int_0^\infty \tilde{A}(k^2; t) k^2 dk \quad (t \gg \tau_s). \quad (\text{A15})$$

Reconsidering Eq. (A10) for $\tilde{\mathbf{r}} = \mathbf{r}' - \mathbf{r} = 0$ and assuming isotropic systems lead to

$$\tilde{W}(0; t) = \frac{1}{2\pi^2} \int_0^\infty \tilde{A}(k^2; t) k^2 dk. \quad (\text{A16})$$

From Eqs. (A15) and (A16), we thus obtain

$$A_p(t) = \frac{4\pi}{9} n \tilde{W}(0; t). \quad (\text{A17})$$

The propagator $\tilde{W}(0; t)$ has a clear physical meaning: It is the probability density that the distance of two spins on different molecules remains stationary or is reestablished by diffusion after an interval t . Note also that the time dependent correlation function $A_p(t)$ does not depend on the number l of the components of the relevant spherical harmonics. This is a direct consequence of the mathematical structure of relation (A9), i.e., the isotropy of the system.

Inserting Eqs. (A2)–(A7) and (A17), Eq. (19) results in

$$\frac{1}{T_{1\text{HH}}^{\text{inter}}(\omega_{\text{H}}; \varphi_{\text{H}})} = \left(\frac{\mu_0}{4\pi} \right)^2 \frac{32\pi^2}{45} \gamma_{\text{H}}^4 \hbar^2 I(I+1) \varphi_{\text{H}} \rho \int_0^\infty dt \tilde{W}(0; t) \times [\cos(\omega_{\text{H}} t) + 4 \cos(2\omega_{\text{H}} t)], \quad (\text{A18})$$

where $n = \varphi_{\text{H}} \rho$ and ρ is the hydrogen number density in the system.

The heteronuclear contribution to proton spin-lattice relaxation by dipolar interaction between protons and deuterons can be derived analogously. Instead of Eq. (A1), the starting formula is now

$$\frac{1}{T_{1\text{HD}}^{\text{inter}}(\omega_{\text{H}}; \varphi_{\text{H}})} = \left(\frac{\mu_0}{4\pi} \right)^2 \frac{3}{2} \gamma_{\text{H}}^2 \gamma_{\text{D}}^2 \hbar^2 S(S+1) \times \left\{ \frac{1}{6} j^{(0)}(\omega_{\text{H}} - \omega_{\text{D}}) + j^{(1)}(\omega_{\text{H}}) + \frac{1}{2} j^{(2)}(\omega_{\text{H}} + \omega_{\text{D}}) \right\}, \quad (\text{A19})$$

where $\varphi_{\text{D}} = (1 - \varphi_{\text{H}})$ is the fraction of deuterium. After repeating all the above calculation steps and setting, we arrive at

$$\begin{aligned} \frac{1}{T_{1\text{HD}}^{\text{inter}}(\omega_{\text{H}}; \varphi_{\text{H}})} &= \left(\frac{\mu_0}{4\pi} \right)^2 \frac{3}{2} \gamma_{\text{H}}^2 \gamma_{\text{D}}^2 \hbar^2 S(S+1) \left\{ \frac{1}{6} j^{(0)}(\omega_{\text{H}} - \omega_{\text{D}}) \right. \\ &\quad \left. + j^{(1)}(\omega_{\text{H}}) + \frac{1}{2} j^{(2)}(\omega_{\text{H}} + \omega_{\text{D}}) \right\} \\ &= \left(\frac{\mu_0}{4\pi} \right)^2 \frac{32\pi^2}{45} \gamma_{\text{H}}^2 \gamma_{\text{D}}^2 \hbar^2 S(S+1) \\ &\quad \times (1 - \varphi_{\text{H}}) \rho \int_0^\infty dt \tilde{W}(0; t) \left[\cos(\omega_{\text{H}} t) \right. \\ &\quad \left. + 2 \cos(2\omega_{\text{H}} t) + \frac{1}{3} \cos(\omega_{\text{H}} - \omega_{\text{D}}) \right]. \quad (\text{A20}) \end{aligned}$$

Assuming a Gaussian propagator,

$$\tilde{W}(\mathbf{r};t) = \frac{1}{((2\pi/3)\langle\tilde{r}^2(t)\rangle)^{3/2}} \exp\left\{-\frac{3}{2}\frac{r^2}{\langle\tilde{r}^2(t)\rangle}\right\}, \quad (\text{A21})$$

where $\langle\tilde{r}^2(t)\rangle \equiv \langle(\mathbf{r}-\mathbf{r}')^2\rangle$ is the mean-squared relative displacement in t , leads to

$$\tilde{W}(0;t) = \frac{1}{((2\pi/3)\langle\tilde{r}^2(t)\rangle)^{3/2}}. \quad (\text{A22})$$

After elementary integration and keeping in mind Eq. (1) for $\alpha < 2/3$, the combination of Eqs. (A18) and (A20) with Eq. (A22) leads to

$$\frac{1}{T_{\text{1HH}}^{\text{inter}}(\omega_{\text{H}}; \varphi_{\text{H}})} = \underbrace{\left(\frac{\mu_0}{4\pi}\right)^2 \frac{16\sqrt{\pi}}{5\sqrt{6}} f_1(\alpha) \frac{\gamma_{\text{H}}^4 \hbar^2 I(I+1) \rho_s}{\omega_{\text{H}} \langle\tilde{r}^2(1/\omega_{\text{H}})\rangle^{3/2}}}_{1/T_1^{\text{inter}}(\omega_{\text{H}}; \varphi_{\text{H}}=1)} \varphi_{\text{H}}, \quad (\text{A23})$$

where

$$f_1(\alpha) = \frac{\pi(1 + 2 \times 2^{3\alpha/2})}{2 \cos(3\pi\alpha/4) \Gamma(3\alpha/2)}, \quad (\text{A24})$$

and

$$\begin{aligned} & \frac{1}{T_{\text{1HD}}^{\text{inter}}(\omega_{\text{H}}; \varphi_{\text{H}})} \\ &= (1 - \varphi_{\text{H}}) \left(\frac{\gamma_{\text{D}}}{\gamma_{\text{H}}}\right)^2 \frac{S(S+1)}{I(I+1)} f_2(\alpha) \frac{1}{T_1^{\text{inter}}(\omega_{\text{H}}, \varphi_{\text{H}}=1)}, \quad (\text{A25}) \end{aligned}$$

where

$$f_2(\alpha) = \frac{1 + 2(1 + \gamma_{\text{D}}/\gamma_{\text{H}})^{(3\alpha-2)/2} + (1 - \gamma_{\text{D}}/\gamma_{\text{H}})^{(3\alpha-2)/2}/3}{1 + 2 \times 2^{3\alpha/2}}. \quad (\text{A26})$$

ACKNOWLEDGMENTS

The authors thank Hans Wiringer for assistance in the course of the experiments. This work was supported by the Volkswagen-Stiftung, the Deutsche Forschungsgemeinschaft, and the CRDF Grant Nos. REC-007 and 2006-RI-112.0/001/359.

- ¹R. Kimmich and N. Fatkullin, *Adv. Polym. Sci.* **170**, 1 (2004).
- ²M. Doi and S. F. Edwards, *The Theory of Polymer Dynamics* (Clarendon, Oxford, 1986).
- ³V. N. Pokrovskii, *The Mesoscopic Theory of Polymer Dynamics* (Kluwer, Dordrecht, 2000).
- ⁴V. N. Pokrovskii, *Adv. Polym. Sci.* **154**, 145 (2001).
- ⁵G. Farrher, I. Ardelean, and R. Kimmich, *J. Magn. Reson.* **182**, 215 (2006).
- ⁶R. Metzler and J. Klafter, *Phys. Rep.* **339**, 1 (2000).
- ⁷R. Kimmich and E. Ansaldo, *Prog. Nucl. Magn. Reson. Spectrosc.* **44**, 257 (2004).
- ⁸C. A. Sholl, *J. Phys. C* **14**, 447 (1981).
- ⁹S. Stapf and R. Kimmich, *Mol. Phys.* **92**, 1051 (1997).
- ¹⁰A. Abragam, *The Principles of Nuclear Magnetism* (Clarendon, Oxford, 1961).
- ¹¹R. Kimmich, *Chem. Phys.* **284**, 253 (2002).
- ¹²K. Binder and W. Paul, *J. Polym. Sci., Part B: Polym. Phys.* **35**, 1 (1997).
- ¹³J. S. Schaffer, *J. Chem. Phys.* **103**, 761 (1995).
- ¹⁴J. T. Padding and W. Briels, *J. Chem. Phys.* **117**, 925 (2002).
- ¹⁵E. Fischer, R. Kimmich, and N. Fatkullin, *J. Chem. Phys.* **106**, 9883 (1997).
- ¹⁶I. Ardelean and R. Kimmich, *Annu. Rep. NMR Spectrosc.* **49**, 43 (2003).
- ¹⁷B. Blümich, *NMR Imaging of Materials* (Clarendon, Oxford, 2000).
- ¹⁸J. Kärger and D. M. Ruthven, *Diffusion in Zeolites* (Wiley, New York, 1992).
- ¹⁹R. Kimmich, N. Fatkullin, R.-O. Seitter, and K. Gille, *J. Chem. Phys.* **108**, 2173 (1998).